JOC The Journal of Organic Chemistry

Article

Nitric Oxide Sensing through 1,2,3,4-Oxatriazole Formation from Acylhydrazide: A Kinetic Study

Abu Saleh Musha Islam, Rahul Bhowmick, Bidhan Chandra Garain, Atul Katarkar, and Mahammad Ali

J. Org. Chem., **Just Accepted Manuscript** • DOI: 10.1021/acs.joc.8b02110 • Publication Date (Web): 08 Oct 2018

Nitric Oxide Sensing through 1,2,3,4-Oxatriazole Formation from Acylhydrazide: A Kinetic Study

Abu Saleh Musha Islam[†], Rahul Bhowmick[†], Bidhan Chandra Garain[†], Atul Katarkar[‡], and Mahammad Ali[*†]

†Department of Chemistry, Jadavpur University, 188 Raja S.C. Mallick Road, Kolkata 700 032, India.

E-mail: m_ali2062@yahoo.com, mali@chemistry.jdvu.ac.in

‡ Department of Biochemistry, University of Lausanne, Ch. des Boveresses 155, 1066 Epalinges, Switzerland.

ABSTRACT: A simple molecular probe displays highly selective turn-on response towards NO by the unprecedented NO-induced formation of 1,2,3,4-oxatriazole ring exhibiting no interference from various endogenous biomolecules including DHA, AA etc. Kinetics of the reactions between NO and the probe provide a mechanistic insight into the formation of 1,2,3,4-oxatriazole which showed that though initially 1,2,3,4-oxatriazole is formed and extractable in solid form, it exists in equilibrium with ring opened azide form which ultimately hydrolysed and converted to carboxylic acid and nitrate. The reaction displays second-order dependence on [NO] and first-order on [Probe]. The probe is water soluble, cell permeable and non-cytotoxic and appropriates for live cell imaging. This constitutes the first report where, there is a direct evidence of NO-induced ring closing reaction of acyl hydrazide moiety leading to the formation of 1,2,3,4-oxatriazole.

INTRODUCTION

Nitric oxide (NO) is an extra- and intracellular messenger molecule mediating diverse signaling pathways in target cells. It plays important roles in many physiological processes that include neuronal signaling, inflammatory response, modulation of ion channels, immune response, phagocytic defense mechanism, penile erection, cardiovascular homeostasis and decompensation in atherogenesis.[1] Depending upon the location and concentration, NO plays major roles in cardiovascular system and central and peripheral nervous systems.[2] In contrast, micro molar concentrations of NO not only forms the reactive nitrogen species (RNS) leading to neurodegenerative disorders and carcinogenesis, but also provides a defense against invading pathogens.[3,4] NO, a diatomic free radical, undergoes a variety of reactions with other radicals in tissues, generating highly reactive nitrosating species involved in nitrosation or oxidation of zinc finger-containing proteins in DNA repair.[5]

NO being lipid-soluble, highly reactive and easily diffuseable in cells and tissues makes it difficult to capture and detect. Several methods, like, chemiluminecence, electrochemical, fluorescence and EPR etc. have been proved to be useful for the *in vitro* and *in vivo* analysis of NO.[6-15] In view of sensitivity, selectivity, spatiotemporal resolution, fluorescence technique is considered as the most favorable method for the detection of endogenous NO. There are a number of inorganic and small organic fluorescent NO probes, many of which are involved in the reaction of aromatic diamines with NO/O_2 forming an electron deficient triazole moiety, that modules the PET (photo induced electron transfer) mechanism and another is oxidative deamination process.[16] However, it exhibits some unexpected limitations which include: (a) oxidation of aromatic diamines and (b) reactions with other reactive oxygen/nitrogen species. All these may result with the generation of fluorescent species.[16-24] Another important methods of NO sensing involve oxidative deamination of aromatic amines, diazotization leading to ring formation and N-nitrosation.[25-39]

Very recently, we have synthesized a thiosemicarbazide containing moiety for the selective detection of NO. Where, thiosemicarbazide group reacts with NO/O_2 to form 1,3,4-oxadiazole and eliminates thionitrous acid.[40] Acylhydrazide, an important organic intermediate, is used in the pharmaceutical industry for the synthesis of nifuratrone.[41] Protein and carbohydrate chemistry routinely utilizes hydrazide functionality. [42] Hydrazides are also used in the modification of oligonucleotides.[43]

Herein, we have developed a new acylhydrazide based molecular probes for NO detection in an oxygenated aqueous medium leading to the formation of 1,2,3,4-oxatriazole ring without any interference by ascorbic acid (AA), dehydroascorbic acid (DHA) or other reactive nitrogen (RNS) and Oxygen (ROS) species. Previously, it was reported [44,45] that 1,2,3,4-oxatriazole moiety may be formed from acyl hydrazide by the reaction with $NaNO_2$ in strongly acidic medium; however, this constitutes the first report where a direct reaction between NO and acyl hydrazide leads to 1,2,3,4-oxatriazole in quantitative yield under the physiological pH conditions at very low (micro molar range) concentration. Detailed kinetic studies and product analysis shed some light on the mechanism of such reaction. Moreover, aqueous solubility makes it a

potent molecular probe for *in vitro* application for monitoring nitric oxide.

RESULTS AND DISCUSSION

The receptor (quinolin-8-yloxy)-acetic acid hydrazide (QAH) was synthesized in two steps. In the initial step (quinolin-8-yloxy)-acetic acid ethyl ester was synthesized from a reaction between 8-hydroxyquinoline and ethyl bromoacetate in 1:1 mole ratio in dry acetone in the presence of anhydrous K_2CO_3. In the second step, ester was reacted with hydrazine hydrate under reflux to afford white coloured QAH (**Scheme 1**). The pure material was characterized by ^{1}H-NMR (**Figure S1**), ^{13}C{^{1}H}-NMR (**Figure S2**), HRMS (**Figure S3**) and FTIR (**Figure S4**) studies.

Scheme 1. Synthetic route of QAH

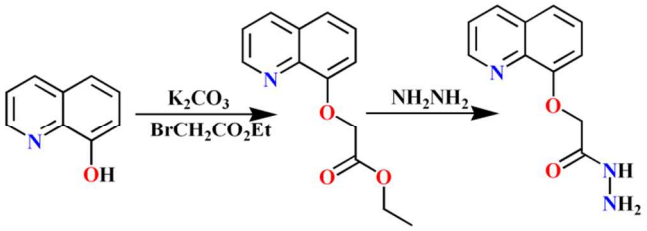

The QAH in aerated aqueous buffer was found to display a highly sensitive and selective fluorogenic response towards NO. The idea of inclusion of 8-hydroxyquinoline as fluorophore unit comes from the fact that it is an important moiety in many biological activities.

Mechanism of fluorescence response of receptor QAH to NO. The PET-ON effect from the high electron rich hydrazide group to the quinoline fluorophore makes parent compound QAH very weakly fluorescent. However, due to the formation of electron deficient 1,2,3,4-oxatriazole moiety out of the reaction between QAH and NO in aerated water, the PET process is blocked. (**Scheme 2**) (*vide infra*). As a result, a remarkable turn-on fluorescence response is observed at λ_{ex} = 380 nm (**Figure 1**).

Scheme 2. Schematic presentation of the PET effect towards Fluorescence response of QAH on interaction with NO/O_2.

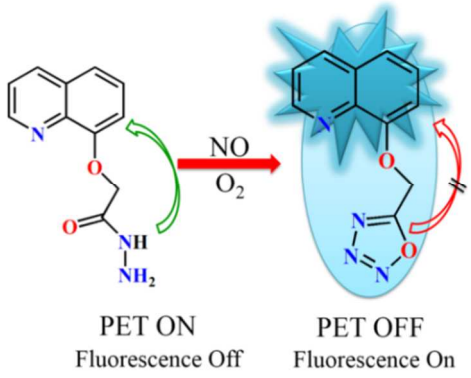

Spectral Response of QAH toward NO. The K_f (apparent formation constant) for the reaction between QAH and NO was calculated by the fluorescence titration method maintaining fixed QAH concentration at 20 μM and varied the NO concentrations between 0 - 40.0 μM in aqueous HEPES buffer at 25 °C. A regular enhancement of an emission peak at ~490 nm was observed with the incremental addition of NO leading to a 23-fold fluorescence enhancement with λ_{ex} = 380 nm (**Figure 1**). We have also performed the excitation wavelength variation study, where approximately fourteen and seven fold of fluorescence enhancements were observed when QAH was excited at 400 and 410 nm respectively, in the presence of excess NO. It is sufficiently high for the detection of NO and also for the intracellular applications (**Figure S5**).

An excellent linear curve was obtained on plotting FI as a function of [NO] up to 40 μM. On further addition of NO the FI remains almost unaltered. The linear part was analyzed using [46] **eqn. 1.**

$$y = \frac{a+b\times c\times x^n}{1+c\times x^n} \quad (1)$$

Where a and b are FIs of the free probe and in the presence of excess NO (≥ 40 μM), c = K_f. Assuming 1>> c*x and n = 1 **eqn. 1.** turns to y= a+b*c*x. The b*c corresponds to the slope of the curve, which ultimately gives c = K_f = (3.01 ± 0.15) x 10^4 M^{-1}.

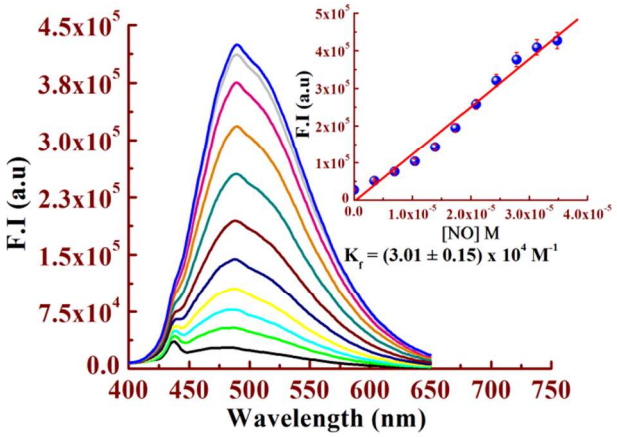

Figure 1. Fluorescence spectra of QAH (20 μM) upon reaction with various amounts of NO (0-40 μM) in 10 mM HEPES buffer (pH 7.20, μ = 0.10 M NaCl at 25 °C, λ_{ex} = 380 nm). Inset is the plot of FI vs. [NO] (S.D. = ±3).

To shed some light on the mechanism of fluorescence enhancement for the reaction between QAH and NO we have isolated the product of the reaction and characterized by exploiting different spectroscopic techniques. Here, QAH (5 mmole) was reacted with nitric oxide in acetonitrile in open air and the light yellow product was isolated and purified by recrystallization from ethanol and elucidated by NMR (**Figures S6 and S7**) (in DMSO-d_6), HRMS (**Figure S8**) and FTIR (**Figure S9**) spectrometry. The ESI-MS^+ peak at 248.0983 (1,2,3,4-

oxatriazole+H_3O^+) clearly suggest the formation of 1,2,3,4-oxatriazole (QOT). The receptor QAH showed IR absorption bands at 3321 cm^{-1}, 3136 cm^{-1} and 1660 cm^{-1} corresponding to -NH_2, -NH and -C=O stretching vibrations, respectively. The product (QOT) showed -C=N and -N=N frequencies at 1679 cm^{-1} and 1646 cm^{-1} respectively devoiding any peaks for -NH_2, -NH and -C=O groups. Thus, it clearly demonstrates that on reaction with NO, IR peaks corresponding to -C=O in QAH is replaced by new peaks for -C=N and -N=N at 1679 cm^{-1} and 1646 cm^{-1} (sym.) respectively in QOT [44,45] (**Figure S9**) signifying the formation of 1,2,3,4-oxatriazole. The $^{13}C\{^1H\}$-NMR studies also support this fact showing a shift in -C=O and -OCH_2 (167.3 and 68.7 ppm) signals of QAH to 170.1 and 66.2 ppm for -C=N and -OCH_2 carbon atom in the QOT. Also from the ^{1}H-NMR titration in CD_3CN it showed that with increasing the concentration of NO the peak corresponding to –NH_2 (4.04 ppm) and –NH (9.38 ppm) of the probe (QAH) gradually diminishes (**Figure S10**) and ultimately vanishes to the base line. We run another IR spectrum after few days of isolation of the product QOT; a very small peak at 2073 cm^{-1} is observed due to the opening of the oxatriazole ring and formation of a very small quantity of azide product (**Figure S11**). We attempted to grow single crystals of QOT in CH_3CN and after one month single crystals of the hydrolysis product of QOT was formed which was characterized by single crystal X-ray diffraction studies (**Figure 2**). So with time QOT is converted to carboxylic acid very slowly through the intermediate azide form[47] (**Scheme 3**). We also studied the stability of the probe (QAH) in CD_3CN and D_2O (1:99 v/v) by ^{1}H-NMR study. After 24 hrs. no observable change in ^{1}H-NMR spectra (**Figure S12**) was noticed. So the sensor QAH is stable in pure water, at least for 24 h.

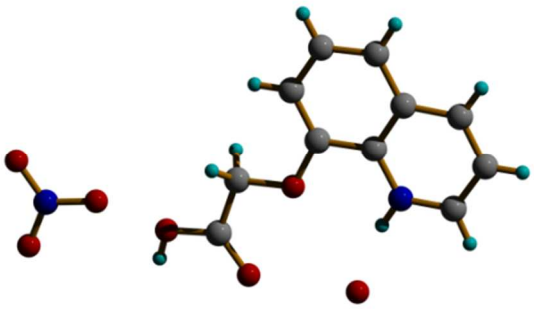

Figure 2. Molecular view of 8-Carboxymethoxyquinolinium ion.

Fluorometric Kinetic Studies. Pseudo-first-order conditions were maintained for the kinetic studies of the reaction of QAH with aqueous NO at pH 7.2 and 15 °C by keeping QAH at 5 μM and NO concentration was varied in the range 30-170 μM (**Figure 3**). The time dependent fluorescence response and corresponding growth curve for [QAH] = 5.0 μM and [NO] = 10 μM at 15 °C is illustrated in **Figure S13.** The kinetic traces at 490 nm display single exponential growth curves which clearly manifest a first-order dependence of rate on [QAH]. The k_{obs} (pseudo-first-order rate constants) were extracted by the grafit program.

When we plot k_{obs} vs. [NO] it yields a non-linear curve with an upward curvature. However, when we plot k_{obs} as a function of $[NO]^2$ it gives an excellent straight line indicating [NO] dependent second-order kinetics (**Figure 3**) which was further confirmed by a plot of log(k_{obs}) vs. log[NO] yielding a slope = (2.2± 0.03) (**Figure S14**) with R = 0.999. In a second experiment, we have determined the dependence of rate on [QAH]. Here the [QAH] was varied ranging between 20–100 μM w.r.t fixed [NO] i.e. 5 μM. A plot of logk_{obs} vs. log[QAH] gives slope (1.00 ± 0.26) (**Figure S15**) with R = 0.997, which also clearly indicates [QAH] dependent first-order kinetics.

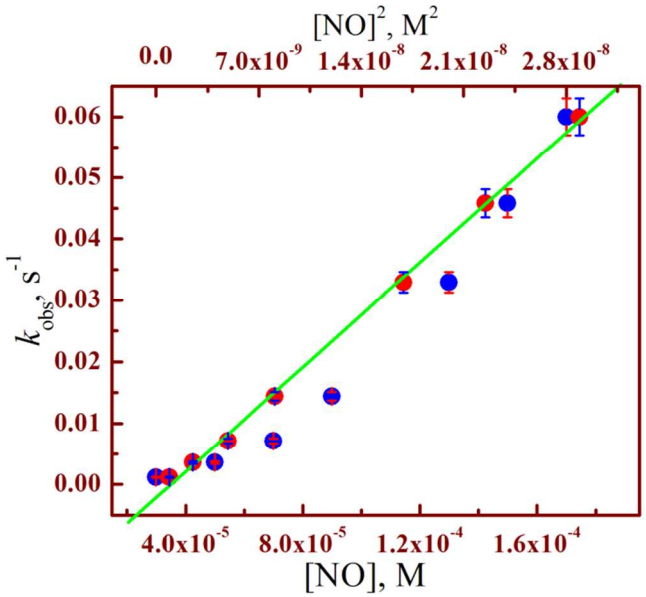

Figure 3. Plots of k_{obs} vs. [NO] (Blue) and $[NO]^2$ (Red) represents the reaction among QAH and NO. Conditions are: [QAH] = 5 μM and [NO] = (30 to 170) μM, 10 mM HEPES buffer (pH = 7.2 , NaCl = 0.10 M, temperature = 15 °C) employing fluorimetric techniques (S.D. = ±3).

Tentative reaction sequences can be framed as:

$$2NO + O_2 \xrightarrow{k_1} 2NO_2 \quad (2)$$

$$NO_2 + NO \xrightarrow{k_2} N_2O_3 \quad (3)$$

$$N_2O_3 + H_2O \xrightarrow{k_3} 2H^+ + 2NO_2^- \quad (4)$$

$$N_2O_3 + L \xrightarrow{k_4} L - NO + NO_2^- + H^+ \quad (5)$$

$$L - NO + H^+ \xrightarrow{fast} L' + H_2O \quad (6)$$

In the eqn (3) N_2O_3 is formed which act as a NO^+ donor and react with L (QAH) to form L-NO, which leads to the formation of the ring-closed 1,2,3,4-oxatriazole moiety (L') (**Scheme 3**). The reported rate constants for the above reactions are: k_1 = 6.33 x 10^6 $M^{-2}s^{-1}$,[48] k_2= 1.1 x10^9 $M^{-1}s^{-1}$,[49] $k_3[H_2O]$ = 1.6 x 10^3 s^{-1},[50]. It clearly indicates that small concentration of NO_2 and N_2O_3 are present as reactive intermediates.

Scheme 3. The proposed mechanism of the reaction of QAH with NO/O_2.

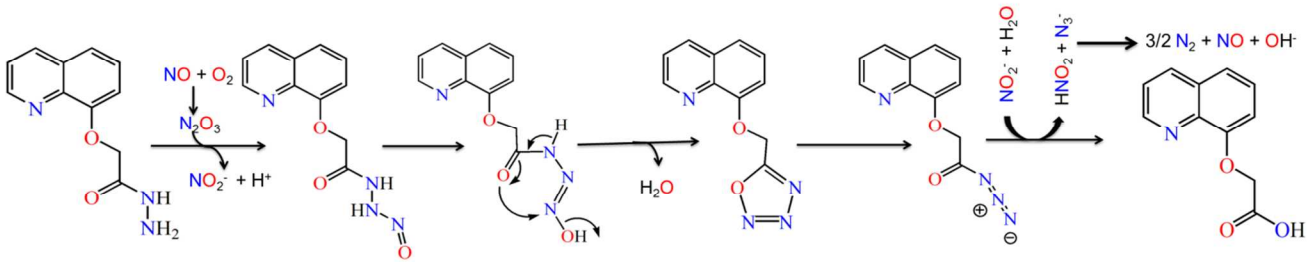

Employing steady-state approximation for the concentration of NO_2 and N_2O_3 eqn (7)[51] can be derived for the formation of QOT (L′).

$$\frac{d[L']}{dt} = \frac{k_1 k_4 [L]}{2(k_3[H_2O] + k_4[L]} [NO]_t^2[O_2]_t \qquad (7)$$

Experimentally, we observed that the reaction rate is second-order in [NO] and first-order on [L] (QAH) which helps us to assume that $k_3[H_2O] >> k_4[L]$ and eqn. (7) turns to (8).

$$\frac{d[L']}{dt} = \frac{k_1 k_4 [L]}{2 k_3[H_2O]} [NO]_t^2[O_2]_t \qquad (8)$$

Adoption of pseudo-first-order conditions with L as a minor component and in open air (the dissolved $[O_2]_t$ = 2.5 mM at 25 °C) reduces eqn. (8) to eqn (9), where k_{obs} = {d[L']/dt}/[L].

$$k_{obs} = k' [NO]_t^2 \qquad (9)$$

Where,

$$k' = \frac{k_1 k_4}{2 k_3[H_2O]} [O_2]_t \qquad (10)$$

The k' = (2.13 × 0.03) x 10^6 $M^{-2}s^{-1}$ at 15 °C was extracted from a linear curve fitting of the plot of k_{obs} vs. $[NO]^2$. With the help of reported values of k_1, $k_3[H_2O]$, and k', the value of k_4 = 4.31 × 10^5 $M^{-1}s^{-1}$ was calculated and revealed same order of magnitude for the alike reactions between N_2O_3 and different thiols:, GSH (2.9 × 10^5 $M^{-1}s^{-1}$), N-acetyl cystein (1.5 × 10^5 $M^{-1}s^{-1}$), HSA (0.3 × 10^5 $M^{-1}s^{-1}$), Cys (2.6 × 10^5 $M^{-1}s^{-1}$), BSA (0.06 × 10^5 $M^{-1}s^{-1}$)[51] and also to our previous results [40].

Selectivity studies. The high specificity of the probe (QAH) toward NO was determined by detecting its fluorescence signal to a variety of reactive species, biomolecules, ROS, RNS and other species (50 μM) such as O^{2-} ,H_2O_2, NO_3^-, •OH, NO_2^-, $ONOO^-$, TEMPO, HCHO, glutathione (GSH), dehydroascorbic acid (DHA), ascorbic acid (AA) and HNO. **Figure 4** clearly highlights that no detectable fluorescence signal of these reagents towards QAH were observed under the identical reaction conditions. Various inorganic anions (**Figures S16(a) and S16(b)**) and cations (**Figures S17(a) and S17(b)**) also do not interfere with the detection of NO.

Determination of LOD (Limit of Detection) for NO and Quantum yields. The 3σ method was used to determine the LOD of NO which was become 45.4 nM (**Figure S18**). The quantum yields (*Φ*) of QAH and QOT are 0.0179 and 0.3759 respectively, with an aqueous acidic solution of quinine sulphate as standard, indicating **QAH** as an example of ideal chemosensor for NO. As in macrophase cultures [52] the typical concentrations of NO is in micro- to nanomolar range; our determined LOD value clearly suggests that the present probe could be successfully used for the measurement of NO in these cell types.

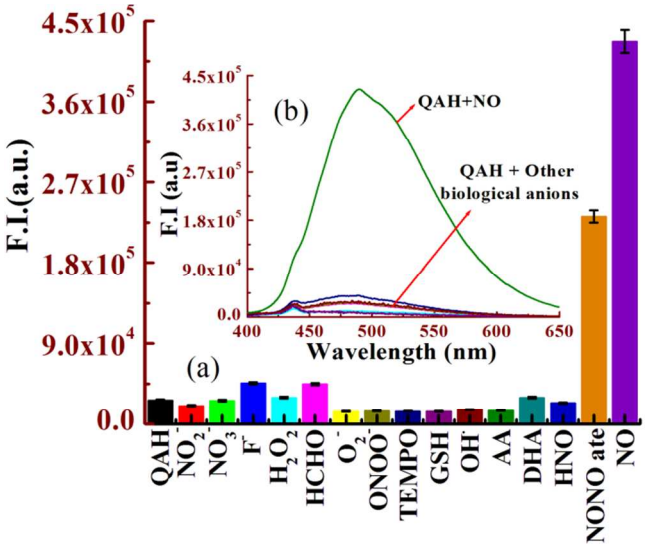

Figure 4. (a) Bar plot and (b) spectral plot of fluorescence responses for the probe QAH at 490 nm towards different reactive species. Conditions: HEPES buffer (10 mM, pH 7.2.); QAH = 20 μM, X^{n-} = 50 μM; λ_{ex} = 380 nm (S.D. = ±3).

pH-Study: To check the practical applicability of the probe under physiological conditions the dependence of fluorescence intensities of QAH and QOT, formed after reaction with NO, were investigated at different pH. The results showed that the probe (10 μM) is very weakly emissive in the pH range 4.0-9.0. But, in the presence of 20 μM of NO the FI was found to be significantly high compared to QAH in the range pH 4.0-8.0 and then FI abruptly decreases with pH (**Figure S19**). This observation clearly indicates that the FI of QOT remains sufficiently high at pH~7.0, implying the safe use of QAH for monitoring NO under physiological conditions.

Probing of PET process by DFT calculations: To confirm the PET process we have carried out the theoretical calculations on QAH and QOT using density functional theory (DFT). The ground state optimized geometries QAH and QOT are found to be stable without any imaginary frequency. The QAH comprises of donor (hydrazide group) and acceptor (quinoline) groups while QOT consists of donor (1,2,3,4- oxatriazole group) and fluorophore (quinoline moiety)[53-56] as based on the orbital distribution diagram. So from the optimized ground state geometries of QAH and QOT, we picked up the orbitals in which the electron distributions are mainly located in the fluorophore (acceptor) part. Similarly, we picked up the orbitals in which the electron distributions are located in orbitals of donor part (**Figure 5**). From **Figure 5(a)** for QAH the HOMO energy of donor (hydrazide moiety) is found to be -8.72 eV, whereas, in the case of fluorophore the HOMO and LUMO energies are -8.90 eV and -0.64 eV, respectively. As a result, HOMO energy of donor (hydrazide moiety) (-8.72 eV) is higher than HOMO energy of the fluorophore, therefore PET process can easily be happened. But in QOT, formed after the reaction of QAH with NO, the HOMO energy level of the donor is lower (-10.92 eV) than HOMO energy of fluorophore (-8.77 eV) (**Figure 5(b)**. Thus, the PET process is blocked, which results in significant enhancement of the fluorescence intensity.

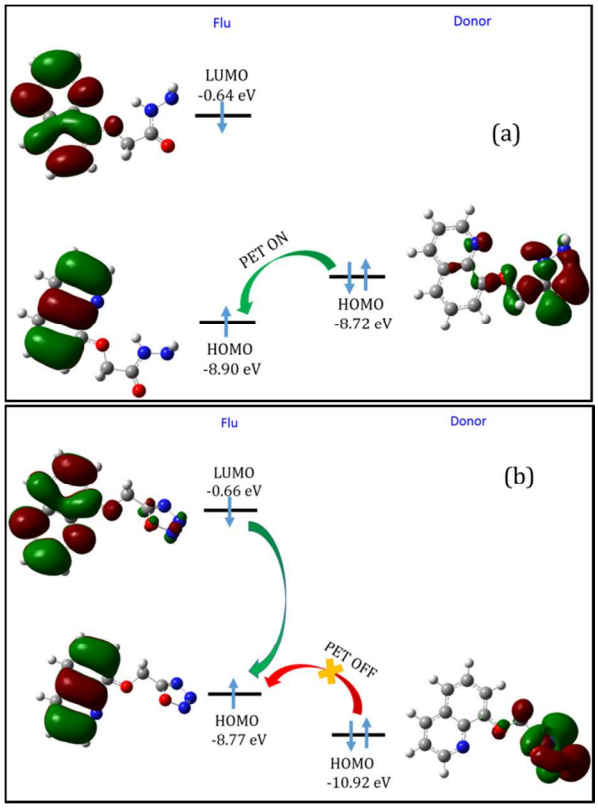

Figure 5. Geometries and orbits of (a) **QAH** and (b) **QOT** derived by DFT calculation. (DFT in CAM-B3LYP/6-31+G (d) level).

Fluorescence cell imaging of NO (Exogenous and Endogenous) in Live Cells. The cytotoxicity of the QAH was evaluated in A549 and Raw 264.7 cells (**Figure 6a**). Both the cell lines exhibited good tolerability, which construes QAH as a biocompatible NO sensor in live cells. Before proceeds with fluorescence imaging, A549 and Raw 264.7 cells were evaluated for exogenously and endogenously release of NO by Griess assay (**Figure 6b-c**).

Endogenously induced NO sensing of QAH was evaluated in Raw 264.7 murin macrophage cells. The cells were co-stimulated with LPS (1.0 mg/mL) and IFN-γ (1000 U/mL) for 2, 4 and 6h followed by QAH (5 μM). Stimulated cells show bright blue fluorescence on treatment with QAH compared to non-stimulated cells (**Figure 7**). The bright blue fluorescence is due to endogenous NO and was confirmed by further incubation of Raw 264.7 cells with NO scavenger PTIO (200 mM) for 2h and then treated with QAH (5 μM) for 30 min, which showed a marked covered up of blue fluorescence, implying that the intracellular fluorescence changes are unquestionably due to NO generation (**Figure 7**). Likely, bright blue fluorescence was seen on exogenously induced NO from DEA-NONOate in the A549 cells (**Figure 8**). The fluorescence intensity due to turn-on signal $(QAH+NO)_f$ were quantified in endogenously and exogenously stimulated NO (**Figure 9 a and b**). Eventually, we have also investigated the detrimental toxic effect of QOT, the product of the reaction between QAH and NO, on the cell viability.

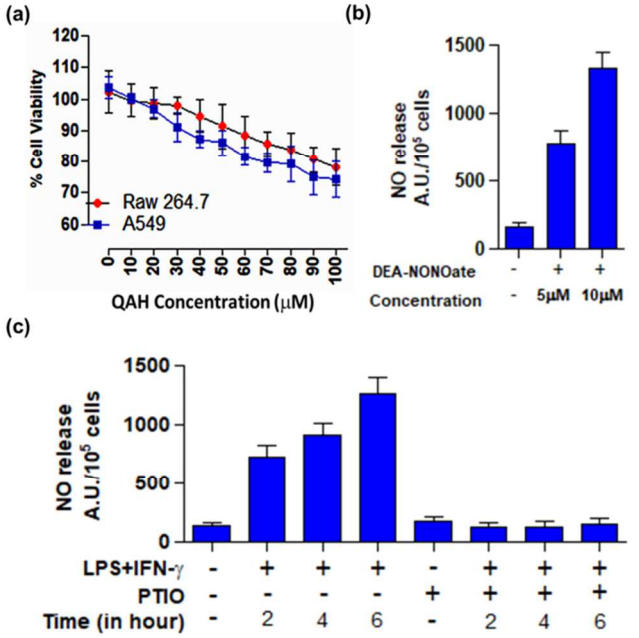

Figure 6. (a) Graphical presentation of assay for Cell viability. (b) Graphical representation (Mean ± SD) of exogenous NO level measurement by Griess assay after adding DEA NONOate 5 and 10 μM. (c) Graphical representation (Mean ± SD) of endogenous measurement of NO level by Griess assay after NO inducer treatment along with iNOS inhibitor PTIO compared to control after 6 h.

The time-dependent cell viability of **QOT** generated from the reaction between **QAH** + DEA-NONOate donor (5 and 10 μM) on A549 cells and -/+ stimulated Raw 264.7 cells up to 12 h does not exhibit any significant change in time-dependent toxicity (**Figure S20**). All these observa-

tions point out the excellent biocompatibility and aptness of **QAH** for the recognition of NO in live cells by fluorescence technique.

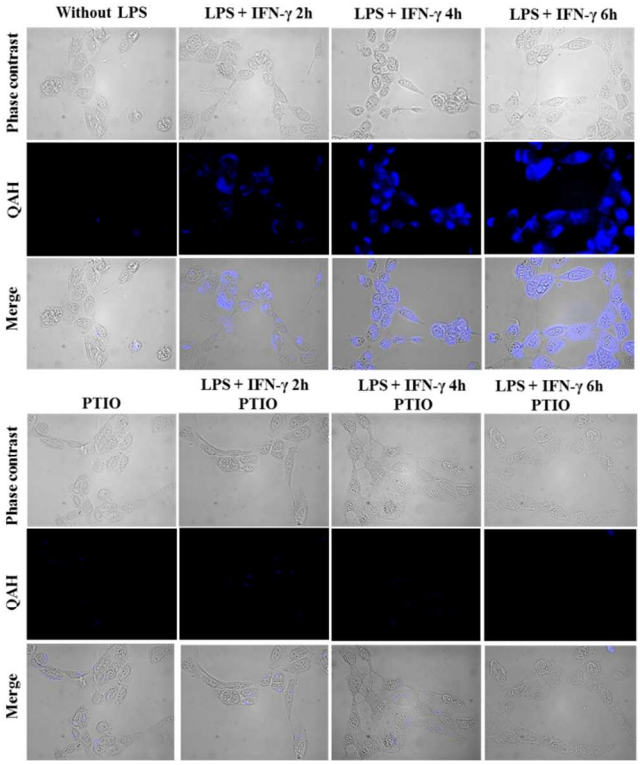

Figure 7. Fluorescence cell image of Raw 264.7 macrophage cells stimulated with LPS (1.0 mg/mL) + IFN-γ (1000 U/mL) with or without iNOS inhibitor PTIO (200 mM) for 2h, 4h and 6h followed by QAH (5 μM) for 30 min. Intracellular blue fluorescence was observed in response to NO interaction with QAH and all the Images were captured at 40X objective.

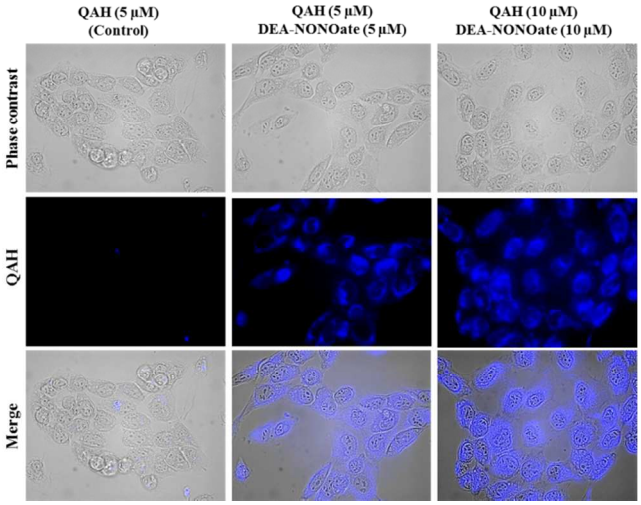

Figure 8. Fluorescence imaging of A549 cells incubated with DEA-NONOate (5 and 10 μM) and QAH (5 and 10 μM). Intracellular blue fluorescence was observed in response NO interaction with **QAH**. Images were taken at 40X objective.

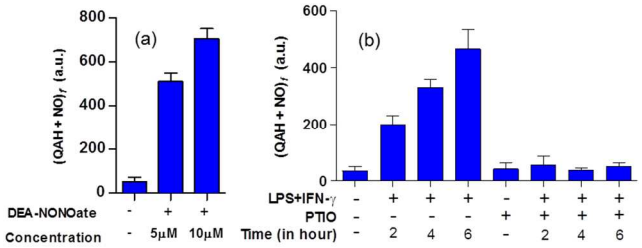

Figure 9. (a) Quantified fluorescence (Mean ± SD) turn-on in A549 cells after treatment with NO donor DEA-NONOate in presence of QAH (b) Quantified fluorescence (Mean ± SD) turn-on in Raw 264.7 cells after stimulation with LPS (1.0 mg/mL) and IFN-γ (1000 U/mL) for 2h, 4h and 6h in presence of QAH (5 μM) with or without iNOS inhibitor PTIO compared to control. (a.u.) = Arbitrary unit.

CONCLUSION

In summary, we have successfully developed a simple acyl hydrazide based fluorescent probe (QAH) for NO sensing in purely aqueous medium. It detects exogenous NO in A549 cells and endogenously generated NO in RAW 264.7 cells. Moreover, the low cytotoxicity, high selectivity, water solubility and excellent detection limit of QAH probe towards NO make it a potential bio imaging probe for *in vitro* monitoring of NO. To the best of our knowledge, this is the first fluorescent probe (QAH) for the detection of NO, through a novel mechanism that leads to the formation of 1,2,3,4-oxatriazole heterocyclic moiety. **Table S1** has been prepared for highlighting of LOD, reaction mechanism and kinetic studies of some published NO probe. The kinetic studies of the reactions between the probe and NO provide a mechanistic insight into the formation of 1,2,3,4-oxatriazole which showed that though initially 1,2,3,4-oxatriazole formed and extractable in solid form, it exists in equilibrium with its ring opened azide form which ultimately hydrolyzed and converted to carboxylic acid and nitrate.

EXPERIMENTAL PROCEDURES

Materials and Methods: The reagent grade starting materials such as Hydrazine hydrate, Ethyl-bromoacetate, 8-Hydroxyquinoline (Sigma Aldrich), salts of K^+, Na^+, Ca^{2+}, Mg^{2+}, Cr^{3+}, Al^{3+}, Fe^{2+}, Mn^{2+}, Fe^{3+}, Cu^{2+}, Co^{2+}, Ni^{2+}, Hg^{2+}, Zn^{2+}, Pb^{2+}, Cd^{2+} etc. and sodium salts of anions like SCN^-, NO_3^-, NO_2^-, N_3^-, I^-, Br^-, F^-, BrO_3^-, HPO_4^-, IO_3^-, OAc^-, $S_2O_3^{2-}$, $S_2O_4^{2-}$, PPi, SCN^-, NCS^- etc. with other reactive species like H_2O_2, •OH, O^{2-},TEMPO, NO_3^-, NO_2^-, $ONOO^-$, GSH, ascorbic acid (AA), dehydroascorbic acid (DHA), and DEA-NONOate (sodium salt) were purchased from Sigma Aldrich and used without further purification. Solvents like absolute ethanol, MeOH, CH_3CN etc. (Merck, India) were of reagent grade and dried before use.

Physical Measurements: FTIR (Fourier Transform Infrared Spectra) (4000 – 400 cm^{-1}) of the ligands (QAH) and product (QOT) of the reaction with NO were recorded on a Perkin-Elmer RX I FTIR spectrophotometer on

solid KBr discs. UV-Vis spectra were recorded on an Agilent 8453 Diode-array spectrophotometer. PTI (Model QM-40) spectrofluorimeter was used for fluorescence studies. Bruker 300 MHz spectrometer was used to run ^1H and $^{13}C\{^1H\}$-NMR spectra in CD_3CN and DMSO-d_6 using trimethylsilane (δ = 0) as an internal standard. ESI-MS^+ (m/z) of the probe (hereafter designated as QAH) and the reaction product (hereafter designated as QOT) were recorded on a HRMS spectrometer (Model: QTof Micro YA263).

Preparation of Stock Solutions: 10 ml of 1.0 x 10^{-3} M stock solution of the probe (QAH) was prepared by dissolving it in two drops of CH_3CN (~1%) and then volume was adjusted with H_2O (HPLC grade). Nitric oxide gas, was purified by passing through solid NaOH pellets,[57] and then purzed through deoxygenated deionized water for 15 min in a sealed vial, which results in NO concentration of 1.74 x 10^{-3} M. The reported method was used to prepare solutions of •OH and $ONOO^-$.[58] Angeli's salt was used a source of HNO.[59] The stock solutions (1.0 x 10^{-3} M) of different cations, anions and different molecular species were prepared in H_2O. All the experiments were carried out in 10.0 mM HEPES buffer at pH 7.2 and ionic strength was maintained at 0.10 M (NaCl). 2.5 ml of the 10.0 mM HEPES buffer was pipetted out into a cuvette and 50 µL of the probe (1.0 x 10^{-3} M) was added, which gives the probe concentration 20 µM, and then variable concentration (0 - 40 µM) of NO was added incrementally and fluorescence spectra were recorded for each solution.

Kinetic Studies: Kinetic studies were carried out under pseudo-first-order conditions with QAH as a minor component (5 µM) and nitric oxide concentration was varied between 30 and 170 µM at pH 7.20, at 15 °C. The dependence of rate on [QAH] was also determined keeping NO as a minor component (5 µM) and [QAH] was varied in the range 20–100 µM. The first-order dependence of rate on [QAH] was confirmed by a plot of logk_{obs} vs. log[QAH] giving a slope (1.00 ± 0.26) with R = 0.999. Similarly a second order dependence on [NO] was confirmed by a plot of logk_{obs} vs. log[NO] with slope (2.2± 0.03) with R = 0.999.

Calculation of LOD: For the LOD (Limit of Detection) calculation of NO 3σ method was used (**eqn. 11**).

$$LOD = 3 \times S_d/S \qquad (11)$$

Where, the standard deviation of the intercept of the blank is represented by S_d and is acquired from a plot of fluorescence intensity (FI) vs. [QAH]. The slope of the linear plot of FI vs. [NO] of the fluorescence titration data is represented by S.

Quantum Yield: Fluorescence quantum yields (Φ) of QAH and QOT were determined with the help of **eqn. 12**

$$\Phi_{smaple} = \frac{OD_{std} \times A_{sample}}{OD_{Sample} \times A_{std}} \times \Phi_{std} \qquad (12)$$

Where, the respective areas of the sample and standard under the fluorescence spectral curves are represented by A_{sample} and A_{std}. The corresponding optical densities of the standard and sample at λ_{ex} are given by OD_{std} and OD_{sample} respectively. Aqueous acidic solution of quininesulfate was used as the standard with Φ_{std} = 0.54.

Computational method: To establish the PET mechanism, the geometry of QAH and QOT were optimized by CAM-B3LYP function using 6-31+G(d) basis set. On the basis of all optimized ground state structures of QAH and QOT, the absorption spectra were calculated by TD-DFT (time-dependent) method applying CAM-B3LYP/6-31+G(d) basis set. All calculations of the molecules were carried out using the Gaussian 09 program package [60] and also PCM (polarizable continuum model) was adopted for solvent (H_2O) effects.

Fluorescence Imaging Experiments:

Cell viability assay: The lung carcinoma A549 cells and Raw 264.7 murine macrophages, grown in Dulbecco's modified Eagle's (DMEM) medium were supplemented with 10% FBS and 1% antibiotic at 37 °C with 5% CO_2. Cell viability of the ligand QAH was evaluated against A549 and Raw 264.7 cells. Briefly, 1×10^5 cells were seeded in 96-well culture plate and allowed to settle down for overnight at 37°C. Cells were then treated with ligands QAH with gradual increasing concentration (ranging 10-100 µM) for 24 h. 10 µl of 3-(4,5-dimethylthiazol-2-yl)-2,5-diphenyltetrazolium bromide (MTT) solution (10 mg/ml 1xPBS) was supplemented to each 96-well and incubated at 37°C for 3 h. Media were removed from all wells and 100 µl acidic isopropyl alcohol was added. The intracellular formazan crystals (blue-violet) were solubilized in 0.04 N acidic isopropyl alcohol and absorbance was measured at 595 nm with a micro plate reader (EMax Precision Micro-Plate Reader, Molecular Devices, USA). Experiments were repeated three times and relative cell viability was expressed as a percentage (%) compared to untreated control cells. Endogenous and exogenous NO generation was measured by Griess assay[61].

In-Vitro Cell incubation and imaging: A549 and Raw 264.7 murine macrophages cells were taken for exogenous and endogenous NO detection respectively. The cells were cultured on glass coverslip inside 35x10 mm culture dishes. Exogenously, A549 cells were treated with sodium salt of nitric oxide donor DEA-NONOate (5 µM and 10 µM) and incubate at 37°C with 5% CO_2 for 30 min and then washed 3 times with 1x PBS followed by treatment with QAH (5 and 10 µM) for 30 min, washed and live cell imaging by fluorescence microscope (Carl Zeiss, Germany) was completed. Endogenously, Raw 264.7 cells were co-stimulated with LPS (1.0 mg/mL) and IFN-γ (1000 U/mL) for 2, 4 and 6 h, and without co-stimulant (con-

trol) and further incubated with QAH (5 μM) for 30 min. The cellular fluorescence was accompanying only with NO generation was confirm by NO scavenger PTIO (2-Phenyl-4,4,5,5-tetramethylimidazoline-1-oxyl-3-oxide) treatment. Raw 264.7 cells were co-stimulated with LPS (1.0 mg/mL) and IFN-γ (1000 U/mL) for 2h, 4h and 6 h, along with PTIO (200 mM) followed by treated with the QAH (5 μM) for 30 min and live fluorescence images were performed.

Syntheses of (Quinolin-8-yloxy)-acetic acid hydrazide (QAH). QAH was synthised in two steps by the literature method.[62] A mixture of 8-hydroxyquinoline (0.06 mol, 8.71 g), ethyl bromoacetate (0.06 mol, 10.02 g) and anhydrous K_2CO_3 (0.06 mol, 8.29 g) in dry acetone was refluxed for 17 h. to afford (quinolin-8-yloxy)-acetic acid ethyl ester. The solid residue thereby formed was removed by filtration and then the solvent was removed under reduced pressure to get the desired product which was purified by column chromatography on silica gel, using ethyl acetate: petroleum ether (1:3) as the yellow oil. Yield 11.79 g (84.6 %).

The resulting ester (0.02 mol, 4.62 g) was dissolved in ethanol to which hydrazine hydrate (0.4 mol) in ethanol was added and the resulting mixture was refluxed on a water bath for 7 h. After cooling, the precipitated solid was filtered and washed with cold water, dried and recrystallized from ethanol (**Scheme 1**). Yield 3.26 g (75%). [$C_{11}H_{11}N_3O_2$]; Molecular Weight 217.0851. ^{1}H-NMR (300 MHz DMSO-d_6): 4.41 (s, 2H, -NH_2), 4.75 (s, 2H, -CH_2), 7.25 (d, 1H), 7.50 - 7.61 (m, 3H, –ArH), 8.38 (d, 1H,–ArH), 8.92 (d, 1H, –ArH), 9.46 (s, 1H, -NH) (**Figure S1**). ^{13}C{^{1}H}-NMR (in DMSO-d_6)(δ, ppm): 167.3, 154.3, 149.8, 140.2, 136.6, 129.6, 127.2, 122.5, 121.4, 112.1, 68.7. (**Figure S2**). ESI-MS^+ (m/z): ($QAH+H^+$) 218.0958 found; calculated 218.0930. (**Figure S3**).

ASSOCIATED CONTENT

Supporting Information.

The Supporting Information is available free of charge on the ACS Publications website at DOI:

Fluorescence and Characterization data of compounds QAH and QOT: ^{1}H NMR,^{13}C-NMR, IR, HRMS, pH effect, DFT computational data, Primary Kinetic data, X-ray crystallography data, CIF file (PDF)

AUTHOR INFORMATION

Corresponding Author

* E-mail: m_ali2062@yahoo.com

‡ Present Address

ORCID

M. Ali: 0000-0003-0756-0468

Notes

The authors declare no competing financial interest.

ACKNOWLEDGMENT

Financial supports from DST (Ref. No. 809(Sanc)/ST/P/S&T/4G-9/2104) West Bengal and CSIR (Ref. 01(2896)/17/EMR-II), New Delhi, India are gratefully acknowledged. Thanks to M. Dolai for helping in crystal data solving.

REFERENCES

(1) O'Dell, T. J.; Hawkins, R. D.; Kandel, E. R. Arancio O. Tests of the roles of two diffusible substances in long-term potentiation: evidence for nitric oxide as a possible early retrograde messenger. *Proc Natl. Acad. Sci. USA* **1991**, *88*, 11285 – 11289.

(2) Butler, A. R.; Williams, D. L. H. The physiological role of nitric oxide. *Chem. Soc. Rev.* **1993**, *22*, 233–241.

(3) Moncada, S.; Palmer, R. M.; Higgs, E. A. Nitric oxide: physiology, pathophysiology, and pharmacology *Pharmacol. Rev*. **1991**, 43, 109-142.;

(4) Conner, E. M.; Grisham, M. B. Nitric Oxide: Biochemistry, Physiology, and Pathophysiology. *Methods Enzymol*. **1995**, 7, 3-13.

(5) Sidorkina O.; Espey M. G.; Miranda K. M.; Wink D. A.; Laval J. Inhibition of Poly(ADP-ribose) Polymerase (PARP) by Nitric Oxide and Reactive Nitrogen Oxide Species. *Free Radical Biol. Med*. **2003**, *35*, 1431–1438

(6) Brune, B.; Dimmeler, S.; Vedia L, M.; Lapetina, E. G. Nitric Oxide: A Signal for ADP-Ribosylation of Proteins. *Life Sci*. **1994**, *54*, 61– 70.

(7) Benjamin, J. P.; Shin, J. H.; Schoenfisch, M. H. Electrochemical nitric oxide sensors for physiological measurements. *Chem. Soc. Rev*. **2010**, *39*, 1925– 1935.

(8) Hu, W.; Boateng, D.; Kong, J.; Zhang, X. Advancement of Fluorescent Methods for Detection of Nitric Oxide. *Austin J. Biosens & Bioelectron*. **2015**, *1*, 1– 9.

(9) Gabe Y.; Urano Y.; Kikuchi K.; Kojima H.; Nagano T. Highly Sensitive Fluorescence Probes for Nitric Oxide Based on Boron Dipyrromethene Chromophore Rational Design of Potentially Useful Bioimaging Fluorescence Probe. *J. Am. Chem. Soc*. **2004**, *126*, 3357–3367.

(10) Sasaki, E.; Kojima H.; Nishimatsu H.; Urano Y.; Kikuchi K.; Hirata Y.; Nagano T. Highly Sensitive Near-Infrared Fluorescent Probes for Nitric Oxide and Their Application to Isolated Organs. *J. Am. Chem. Soc*. **2005**, *127*, 3684–3685.

(11) Yang ,Y.; Seidlits, S. K.; Adams, M. M.; Lynch V. M.; Schmidt, C. E.; Anslyn, E. V.; Shear, J. B. A Highly Selective Low-Background Fluorescent Imaging Agent for Nitric Oxide. *J. Am. Chem. Soc*. **2010,** *132*, 13114–14116.

(12) McQuade, L. E.; Pluth, M. D.; Lippard, S. J. Mechanism of Nitric Oxide Reactivity and Fluorescence Enhancement of the NO-Specific Probe CuFL1. *Inorg. Chem.* **2010**, *49*, 8025–8033.

(13) McQuade, L. E.; Lippard, S. J. Fluorescence-Based Nitric Oxide Sensing by Cu(II) Complexes That Can Be Trapped in Living Cells. *Inorg. Chem.* **2010**, *49*, 7464–7471.

(14) Lim, M. H.; Lippard, S. J. Fluorescence-Based Nitric Oxide Detection by Ruthenium Porphyrin Fluorophore Complexes. *Inorg. Chem.* **2004**, *43*, 6366-6370.

(15) Li, H.; Wan, A. Fluorescent Probes for Real-time Measurement of Nitric Oxide in Living Cells. *Analyst* **2015**, *140*, 7129– 7141.

(16) Beltrán, A.; Burguete, M. I.; Abánades, D. R.; Pérez-Sala, S. D.; Luis, V.; Galindo, F. Turn-on Fluorescent Probes for Nitric Oxide Sensing Based on the *Ortho*-Hydroxyamino Structure Showing no Interference with Dehydroascorbic acid. *Chem. Commun.* **2014**, *50*, 3579–3581.

(17) Lim, M. H.; Lippard, S. J. Copper Complexes for Fluorescence-Based NO Detection in Aqueous Solution. *J. Am. Chem. Soc.* **2005**, *127*, 12170-12171.

(18) Lim, M. H.; Lippard, S. J. Fluorescent Nitric Oxide Detection by Copper Complexes Bearing Anthracenyl and Dansyl Fluorophore Ligands. *Inorg. Chem.* **2006**, *45*, 8980-8989.

(19) Sun, C.; Shi, W.; Song, Y.; Chen, W.; Ma, H. An unprecedented strategy for selective and sensitive fluorescence detection of nitric oxide based on its reaction with a selenide. *Chem. Commun.* **2011**, *47*, 8638–8640.

(20) Smith, R. C.; Tennyson, A. G.; Lim, M. H.; Lippard S. J. Conjugated Polymer-Based Fluorescence Turn-On Sensor for Nitric Oxide. *Org. Lett.* **2005**, *7*, 3573-3575.

(21) Shiue, T. W.; Chen, Y. H.; Wu, C. M.; Singh, G.; Chen, H. Y.; Hung, C. H.; Liaw, W. F.; Wang, Y. M. Nitric Oxide Turn-on Fluorescent Probe Based on Deamination of Aromatic Primary Monoamines. *Inorg. Chem.* **2012**, *51*, 5400–5408.

(22) Kojima, H.; Hirotani, M.; Nakatsubo, N.; Kikuchi, K.; Urano, Y.; Higuchi, T.; Hirata, Y.; Nagano, T. Bioimaging of Nitric Oxide with Fluorescent Indicators Based on the Rhodamine Chromophore. *Anal. Chem.* **2001**, 73, 1967-1973.

(23) Yu, H.; Zhang, X.; Xiao, Y.; Zou, W.; Wang, L.; Jin, L. Targetable Fluorescent Probe for Monitoring Exogenous and Endogenous NO in Mitochondria of Living Cells. *Anal. Chem.* **2013**, *85*, 7076–7084.

(24) Dong, X.; Heo, C. H.; Chen, S.; Kim, H. M.; Liu, Z. Quinoline-Based Two-Photon Fluorescent Probe for Nitric Oxide in Live Cells and Tissues. *Anal. Chem.* **2014**, *86*, 308–311.

(25) Yao, H. W.; Zhu, X. Y.; Guo, X. F.; Wang, H. An Amphiphilic Fluorescent Probe Designed for Extracellular Visualization of Nitric Oxide Released from Living Cells. *Anal. Chem.* **2016**, 88, 9014-9021.

(26) Dai, Z.; Tian, L.; Song, B.; Liu, X.; Yuan, J. Development of a novel lysosome-targetable timegated luminescence probe for ratiometric and luminescence lifetime detection of nitric oxide in vivo. *Chem Sci.* **2017**, *8*, 1969–1976.

(27) Wang, C.; Song, X.; Han, Z.; Li, X.; Xu, Y.; Xiao, Y. Monitoring Nitric Oxide in Subcellular Compartments by Hybrid Probe Based on Rhodamine Spirolactam and SNAP-tag. *ACS Chem. Biol.* **2016**, *11*, 2033-2040.

(28) Mao, Z.; Feng, W.; Li, Z.; Zeng, L.; Lv, W.; Liu, Z. NIR in, far red out: developing a two-photon fluorescent probe for tracking nitric oxide in deep tissue. *Chem. Sci.* **2016**, **7**, 5230-5235.

(29) Tian, L.; Dai, Z.; Liu, X.; Song, B.; Ye, Z.; Yuan, J. Ratiometric Time-Gated Luminescence Probe for Nitric Oxide Based on an Apoferritin-Assembled Lanthanide Complex-Rhodamine Luminescence Resonance Energy Transfer System. *Anal. Chem.* **2015**, *87*, 10878–10885.

(30) Tang, J.; Guo, Z.; Zhang, Y.; Bai, B.; Zhu, W. H. Rational design of a fast and selective near infrared fluorescent probe for targeted monitoring of endogenous nitric oxide. *Chem. Commun.* **2017**, 53, 10520- 10523.

(31) Huo, Y.; Miao, J.; Han, L.; Li, Y.; Li, Z.; Shib, Y.; Guo, W. Selective and sensitive visualization of endogenous nitric oxide in living cells and animals by a Sirhodamine deoxylactam-based near-infrared fluorescent probe. *Chem. Sci.* **2017**, *8*, 6857–6864.

(32) Yu, H.; Zhang, X.; Xiao, Y.; Zou, W.; Wang, L.; Jin, L. Targetable Fluorescent Probe for Monitoring Exogenous and Endogenous NO in Mitochondria of Living Cells. *Anal. Chem.* **2013**, *85*, 7076–7084.

(33) Wang, N.; Yu, X.; Zhang, K.; Mirkin, C. A.; Li, J. Upconversion Nanoprobes for the Ratiometric Luminescent Sensing of Nitric Oxide. *J. Am. Chem. Soc.* **2017**, *139*, 12354–12357.

(34) Huo, Y.; Miao, J.; Li, Y.; Shi, Y.; Shia, H.; Guo, W. Aromatic primary monoamine-based fast-response and highly specific fluorescent probes for imaging the biological signaling molecule nitric oxide in living cells and organisms. *J. Mater. Chem. B*. **2017**, 5, 2483–2490.

(35) Reinhardt, C. J.; Zhou, E. Y.; Jorgensen, M. D.; Partipilo, G.; . Chan, J. A Ratiometric Acoustogenic Probe for in Vivo Imaging of Endogenous Nitric Oxide. *J. Am. Chem. Soc.* **2018**, *140* , 1011–1018.

(36) Mao, Z.; Jiang, H.; Song, X.; Hu, W.; Liu, Z. Development of a Silicon-Rhodamine Based Near-Infrared Emissive Two-Photon Fluorescent Probe for Nitric Oxide. *Anal. Chem.* **2017**, *89*, 9620–9624.

(37) Mia, J.; Huo, Y.; Lv, X.; Li, Z.; Cao, H.; Shi, H.; Shi, Y.; Guo, W. Fast-response and highly selective fluorescent probes for biological signaling molecule NO based on N-nitrosation of electron-rich aromatic secondary amines. *Biomaterials*, **2016**, *78*, 11-19.

(38) Dai, C. G.; Wang, J. L.; Fu,Y. L.; Zhou, H. P.; Song, Q. H. Selective and Real-Time Detection of Nitric Oxide by a Two-Photon Fluorescent Probe in Live Cells and Tissue Slices. *Anal. Chem.,* **2017**, *89*, 10511–10519.

(39) Muthuraj, B.; Deshmukh, R.; Trivedi, V.; Iyer, P. K. Highly Selective Probe Detects Cu^{2+} and Endogenous NO Gas in Living Cell. *ACS Appl. Mater. Interfaces,* **2014**, *6*, 6562–6569.

(40) Islam, A S M.; Bhowmick, R.; Pal, K.; Katarkar, A.; Chaudhuri, K.; Ali, M. A Smart Molecule for Selective Sensing of Nitric Oxide: Conversion of NO to HSNO; Relevance of Biological HSNO Formation. *Inorg. Chem.* **2017**, *56*, 4324-4331.

(41) Marion, L.; Lavigne, R.; Lemay, L. The Stracture of Sedamin. *Can. J. Chem.* **1951**, *29*, 843–847.

(42) Raddatz, S.; Mueller-Ibeler, J.; Kluge, J. L.; Burdinski, G.; Havens, J. R.; Onofrey, T. J.; Wang, D.; Schweitzera, Markus. Hydrazide oligonucleotides: new chemical modification for chip array attachment and conjugation. *Nucleic Acid Res.* **2002**, *21*, 4793–4802.

(43) de Lumley-Woodyear, T.; Campbell ,C. N.; Heller, A. Direct Enzyme-Amplified Electrical Recognition of a 30-Base Model Oligonucleotide. *J. Am. Chem. Soc.* **1996**, *118*, 5504–5505.

(44) Ibrahim, M. K.; Adl, K. E.; Zayed, M. F.; Mahdy, H. A. Design, synthesis, docking, and biological evaluation of some novel 5-chloro-2-substituted sulfanylbenzoxazole derivatives as anticonvulsant agents. *Med. Chem. Res.* **2015**, *24*, 99–114.

(45) Azab, M. E.; Madkour,H. M. F.; Ibraheem, M. A. E. The Utility of 2-(5,6,7,8-Tetrahydrobenzo[b]thieno- [2,3-d]pyrimidin-4-yloxy) Acethydrazide in Heterocyclic Synthesis. *Phosphorus, Sulfur and Silicon* **2006**, *181*, 1299–1313.

(46) Islam, A. S. M.; Alam, R.; Katarkar, A.; Chaudhuri, K.; Ali, M. Di-oxime Based Selective Fluorescent Probe for Arsenate and Arsenite Ions in a Purely Aqueous Medium with Living Cell Imaging Applications and H-bonding Induced Microstructure Formation. *Analyst* **2015**, *140*, 2979-2983.

(47) Wu, C. M.; Chen, Y. H.; Dayananda, K.; Shiue, T. W.; Hung, C. H.; Liaw, W. F.; Chen, P. Y.; Wang, Y. M. Sensitivity evaluation of rhodamine B hydrazide towards nitric oxide and its application for macrophage cells imaging. *Anal. Chem. Acta*. **2011**, *708*, 141–148.

(48) Kharitonov, V. G.; Sundquist, A. R.; Sharma, V. S. Kinetics of nitric oxide autoxidation in aqueous solution. *J. Biol. Chem.* **1994**, *8,* 5881-5883.

(49) Gra¨tzel, M.; Taniguchi, S.; Henglein, A. Pulse radiolytic investigation of the oxidation of NO and of the equilibrium

N_2O_3 ⇄ NO + NO_2 in aqueous solution. *Phys. Chem.* **1970**, *74*, 488–492.

(50) Licht, W. R.; Tannenbaum, S. R.; Deen, W. M. Use of ascorbic acid to inhibit nitrosation: kinetic and mass transfer considerations for an in vitro system. *Carcinogenesis* **1988**, *9*, 365–372.

(51) Kharitonov, V. G.; Sundquist, A. R.; Sharma, V. S. Kinetics of Nitrosation of Thiols by Nitric Oxide in the Presence of Oxygen. *J. Biol. Chem.* **1995**, *270*, 28158–28164.

(52) Chen, T.; Zamora, R.; Zuckerbraun, B.; Billiar, T. R. Role of Nitric Oxide in Liver Injury. *Curr Mol Med*. **2003** , *3*, 519-526.

(53) Zhang,Y. J.; Yang, W. J.; Wang, C. K. Effect of fluorophore on sensing NO for newly synthesized PET-based two-photon fluorescent probes. *Chemical Physics* **2016**, *468*, 37–43.

(54) Xu, Z.; Ren, A. M.; Wang, D.; Guo, J. F.; Feng, J. K.; Yu, X. A theoretical investigation on two latest two-photon pH fluorescent probes. *Journal of Photochemistry and Photobiology A: Chemistry* **2014**, *293*, 50–56.

(55) Xu, Z.; Ren, A. M.; Guo, J. F.; Liu, X. T.; Huang, S.; Feng, J. K. A Theoretical Investigation of Two Typical Two-Photon pH Fluorescent Probes. *Photochemistry and Photobiology* **2013**, *89*, 300–309.

(56) Mao, Z.; Jiang, H.; Song,X.; Hu, W.; Liu, Z. Development of a Silicon-Rhodamine Based Near-Infrared Emissive Two-Photon Fluorescent Probe for Nitric Oxide. *Anal. Chem.* **2017**, *89*, 9620–9624.

(57) Mesároš, Š.; Grunfeld, S.; Mesárošová, A.; Bustin, D.; Malinski, T. Determination of nitric oxide saturated (stock) solution by chronoamperometry on a porphyrine microelectrode. *Anal. Chim. Acta*. **1997**, *339*, 265–270.

(58) Miyamoto, S.; Martinez, G. R.; Martins, A. P. B.; Medeiros, M. H. G.; Di Mascio, P. Direct Evidence of Singlet Molecular Oxygen [O_2 ($1\Delta g$)] Production in the Reaction of Linoleic Acid Hydroperoxide with Peroxynitrite. *J. Am. Chem. Soc.* **2003**, *125*, 4510–4517.

(59) Wrobel, A. T.; Johnstone, T. C.; Liang, A. D.; Lippard, S. J.; Fuentes, P. R. A Fast and Selective Near-Infrared Fluorescent Sensor for Multicolor Imaging of Biological Nitroxyl (HNO). *J. Am. Chem. Soc.* **2014**, *136*, 4697–4705.

(60) M. J. Frisch, G. W. Trucks, H. B. Schlegel, G. E. Scuseria, M. A. Robb, J. R. Cheeseman, G. Scalmani, V. Barone, B. Mennucci, G. A. Petersson, H. Nakatsuji, M. Caricato, X. Li, H. P. Hratchian, A. F. Izmaylov, J. Bloino, G. Zheng, J. L. Sonnenberg, M. Hada, M. Ehara, K. Toyota, R. Fukuda, J. Hasegawa, M. Ishida, T. Nakajima, Y. Honda, O. Kitao, H. Nakai, T. Vreven, J. A. Montgomery Jr., J. E. Peralta, F. Ogliaro, M. Bearpark, J. J. Heyd, E. Brothers, K. N. Kudin, V. N. Staroverov, R. Kobayashi, J. Normand, K. Raghavachari, A. Rendell, J. C. Burant, S. S. Iyengar, J. Tomasi, M. Cossi, N. Rega, J. M. Millam, M. Klene, J. E. Knox, J. B. Cross, V. Bakken, C. Adamo, J. Jaramillo, R. Gomperts, R. E. Stratmann, O. Yazyev, A. J. Austin, R. Cammi, C. Pomelli, J. W. Ochterski, R. L. Martin, K. Morokuma, V. G. Zakrzewski, G. A. Voth, P. Salvador, J. J. Dannenberg, S. Dapprich, A. D. Daniels, O¨. Farkas, J. B. Foresman, J. V. Ortiz, J. Cioslowski and D. J. Fox, *Gaussian 09*, (Revision A.1), Gaussian, Inc., Wallingford, CT, **2009.**

(61) Alam, R.; Islam, A. S. M.; Sasmal, M.; Katarkar, A.; Ali, M. A rhodamine-based turn-on nitric oxide sensor in aqueous medium with endogenous cell imaging: an unusual formation of nitrosohydroxylamine. *Org. Biomol. Chem*. **2018**, *16*, 3910-3920.

(62) Islam, A. S. M.; Bhowmick, R.; Mohammad, H.; Katarkar, A.;Chaudhuri, K.; Ali, M. A Novel 8-hydroxyquinoline-pyrazole Based Highly Sensitive and Selective Al(III) Sensor in a purely Aqueous Medium with Intracellular Application: Experimental and Computational Studies. *New J. Chem.* **2016**, *40*, 4710-4719.

TOC

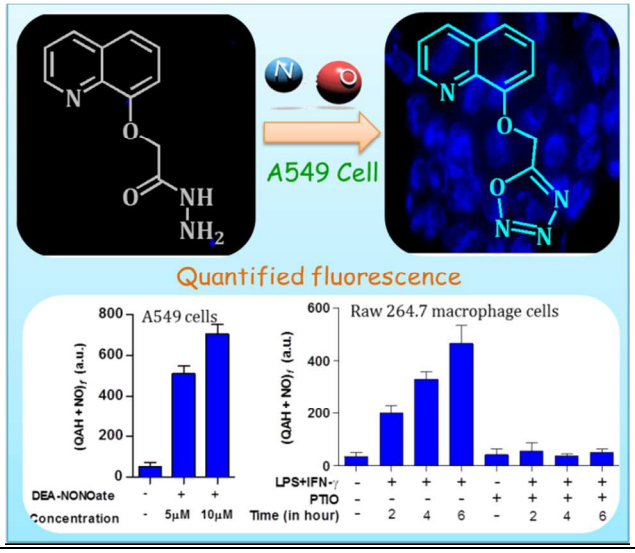
A549 Cell
Quantified fluorescence
A549 cells
Raw 264.7 macrophage cells
(QAH + NO)f (a.u.)
DEA-NONOate
Concentration
5μM
10μM
LPS+IFN-γ
PTIO
Time (in hour)